A Method for Semi-Automatic Segmentation and Evaluation of Intracranial Aneurysms in Bone-Subtraction Computed Tomography Angiography (BSCTA) Images

Susanne Krämer[1], Hendrik Ditt[2], Christina Biermann[3], Michael Lell[4], Jörg Keller[1]

[1]Chair for Parallelism and VLSI, FernUniversität in Hagen, Universitätsstrasse 1, 58084 Hagen, Germany

[2]Siemens Healthcare, Siemensstrasse 1, 91301 Forchheim, Germany

[3]Siemens Healthcare, Siemensstrasse 1, 91301 Forchheim, Germany, and Dept. of Diagnostic Radiology, Eberhard-Karls-University of Tuebingen, Hoppe-Seyler-Str. 3, 72076 Tuebingen, Germany

[4]Institute of Diagnostic Radiology, University of Erlangen-Nuremberg, Maximiliansplatz 1, 91054 Erlangen, Germany

ABSTRACT

The rupture of an intracranial aneurysm has dramatic consequences for the patient. Hence early detection of unruptured aneurysms is of paramount importance. Bone-subtraction computed tomography angiography (BSCTA) has proven to be a powerful tool for detection of aneurysms in particular those located close to the skull base. Most aneurysms though are chance findings in BSCTA scans performed for other reasons. Therefore it is highly desirable to have techniques operating on standard BSCTA scans available which assist radiologists and surgeons in evaluation of intracranial aneurysms. In this paper we present a semi-automatic method for segmentation and assessment of intracranial aneurysms. The only user-interaction required is placement of a marker into the vascular malformation. Termination ensues automatically as soon as the segmentation reaches the vessels which feed the aneurysm. The algorithm is derived from an adaptive region-growing which employs a growth gradient as criterion for termination. Based on this segmentation values of high clinical and prognostic significance, such as volume, minimum and maximum diameter as well as surface of the aneurysm, are calculated automatically. the segmentation itself as well as the calculated diameters are visualised. Further segmentation of the adjoining vessels provides the means for visualisation of the topographical situation of vascular structures associated to the aneurysm. A stereolithographic mesh (STL) can be derived from the surface of the segmented volume. STL together with parameters like the resiliency of vascular wall tissue provide for an accurate wall model of the aneurysm and its associated vascular structures. Consequently the haemodynamic situation in the aneurysm itself and close to it can be assessed by flow modelling. Significant values of haemodynamics such as pressure onto the vascular wall, wall shear stress or pathlines of the blood flow can be computed. Additionally a dynamic flow model can be generated. Thus the presented method supports a better understanding of the clinical situation and assists the evaluation of therapeutic options. Furthermore it contributes to future research addressing intervention planning and prognostic assessment of intracranial aneurysms.

Keywords: Computed Tomography, Bone-Subtraction Computed Tomography Angiography, Aneurysm, Segmentation, Haemodynamics, Flow Modelling

Further author information:
Susanne Krämer: DivingAur@web.de
Hendrik Ditt: Hendrik.Ditt@Siemens.com
Christina Biermann: Christina.Biermann@Siemens.com

1. INTRODUCTION

Depending on the diagnostic approach the incidence of intracranial aneurysms is estimated to range between 3 to 6% of the population[1,2] . Formation and growth of aneurysms as well as their tendency to rupture are affected by various influences. There is also strong evidence that genetic factors are involved in the formation of aneurysms[3] and a familial predisposition has been proved[4] . Furthermore gender and age play a part in the formation and growth of aneurysms, females and older persons are more likely to develop aneurysms[4,5] . Other risk factors include hypertension, atherosclerosis, diabetes, and vascular anatomical differences along with smoking and poor diet[6–8] . These factors also increase the risk for rupture of an aneurysm[9] . A long-term study found that the age of a patient correlates reversely to risk of rupture of an aneurysm and that the relative risk for rupture is 1.11 per mm in diameter of the unruptured aneurysm[10] . About 70 to 85% all of subarachnoid haemorrhages (SAH) are caused by ruptured aneurysms[11,12] and the incidence of SAH linked to rupture of an aneurysm is 6 out of a population of 100,000[3] . The prognosis of an SAH due to a ruptured aneurysm is poor, fatality is about 50% and of the surviving patients about one third remains permanently dependent[11,13] .

Clinically these patients present with symptoms of a stroke. The primary tool for emergency evaluation of stroke patients is computed tomography (CT), including non-enhanced CT scans, CT angiography (CTA) and perfusion CT[14–16] . Yet unruptured aneurysms usually remain undetected unless imaging of the vascular situation in the brain is undertaken for other reasons. Bone-subtraction computed tomography angiography (BSCTA) has become the most important non-invasive method for the evaluation of intracranial vascular structures, in particular of the vessels close to the skull base[17] . However so far no procedures that assist the clinician in the evaluation of intracranial aneurysms on BSCTA images exist. Hence it is desirable to provide specialised tools operating on standard BSCTA images and supporting diagnosis and evaluation of aneurysms.

The goals of this work were to make emphasized visualisation and crucial dimensional values of intracranial aneurysms available to the clincian in a semi-automatic procedure. Additionally modelling of the haemodynamic situation in the aneurysm itself and the affiliated vascular structures was to be facilitated. All computations were to be executed on images produced by standard BSCTA protocols. User interaction was limited to initial marking of the aneurysm only.

In this paper the segmentation algorithm and its criterion for termination are described. Explanations regarding further computations, e.g. that of maximum and minimum diameter, volume and surface of the aneurysm, follow. Consequently the extension of the segmentation process into associated vascular structures is explained. The purpose of this step is to present the clinician a view onto the aneurysm unobstructed by vessels not related to the aneurysm and at the same time retaining the topographical context. Finally computation of haemodynamics in the aneurysm is illustrated. This modelling is facilitated by a stereolithographic (STL) representation of the wall of the aneurysm and associated vessels which is generated based on the entire segmentation.

2. RELATED WORK

As mentioned above most aneurysms are chance-findings in CTA scans performed for other reasons. Vascular structures of the brain can also be segmented in magnetic resonance angiography (MRA)[18] or phase contrast magnetic resonance angiography (PCMRA) images[19,20] . Methods proposed for segmentation of intracranial vessels in these images are for example the capillary active contour model,[21] an approach based on statistical mixture modeling and local phase coherence[22] or the Z-buffer segmentation[22] . These approaches aim to segment the entire vasculature of the brain in the respective images thus enabling detection of aneurysms by the physician but do not provide the means for automatic assessment of aneurysms.

3. BONE-SUBTRACTION CT ANGIOGRAPHY (BSCTA)

A characteristic of intracranial vascular structures is that most vessels of particular interest run in immediate proximity to the osseous skull or are even enclosed into osseous channels. Yet in CTA images greyvalues of bone and contrast-enhanced vessels range in the same interval. Consequently automatic seperation of these two anatomical structures proves to be very difficult. BSCTA however provides an unobstructed presentation of these vascular structures[23–25] . Two separate CT scans are required: a low-dose non-enhanced CT (NECT) scan and

an enhanced CT scan (CTA) of the same region. Bones are detected and masked in the NECT dataset, the so-called bone-mask resulting from this process. In the next step the bone-mask is subtracted from the CTA dataset and thus osseous structures are suppressed. All other tissue values remain unchanged. Motion correction is of major importance as even miniscule patient movements lead to incomplete subtraction of bone in the BSCTA dataset. For this reason a precise alignment of the two datasets is essential to avoid bone artefacts and to retain the vascular structures in their entity. The head is considered to be a rigid body and thus translation and rotation fullfill the requirements for alignment of both datasets. In a slab based approach each slab is aligned separately to account for movements of the patient during one scan. This approach reduces motion artefacts significantly. However isolated motion of bones like the mandible lead to artefacts in the resulting BSCTA dataset as well. An additional partially rigid motion correction amends those areas in the dataset where dislocations were detected[26,27] . Thus BSCTA allows for unobstructed display of vessels and vascular malformations in close proximity to the bone in particular to the skull base. An accurate diagnosis is supported and therapeutic decisions can be evaluated even prior to invasive diagnostic procedures.

4. SEGMENTATION AND EVALUATION OF ANEURYSMS

As mentioned above segmentation and evaluation of intracranial aneurysms is carried out on BSCTA images. For this paper 25 intracranial aneurysms of various shapes, sizes and locations were employed as test data. Size ranged from 7 mm to 32 mm in diameter, saccular, balloon-shaped and asymmetric aneurysms were represented. The aneurysms were located at the Carotissiphon, the Arteria communicans anterior, Arteria cerebri media and the tip of the Arteria basilaris.

4.1 Segmentation

Via a single mouse-click the user sets a start marker (seed) into either a two-dimensional multiplanar reformation (MPR) or a three-dimensional volume rendering technique (VRT) visualisation of the BSCTA (see Fig. 1). This is the only user interaction required for segmentation, visualisation and calculation of values.

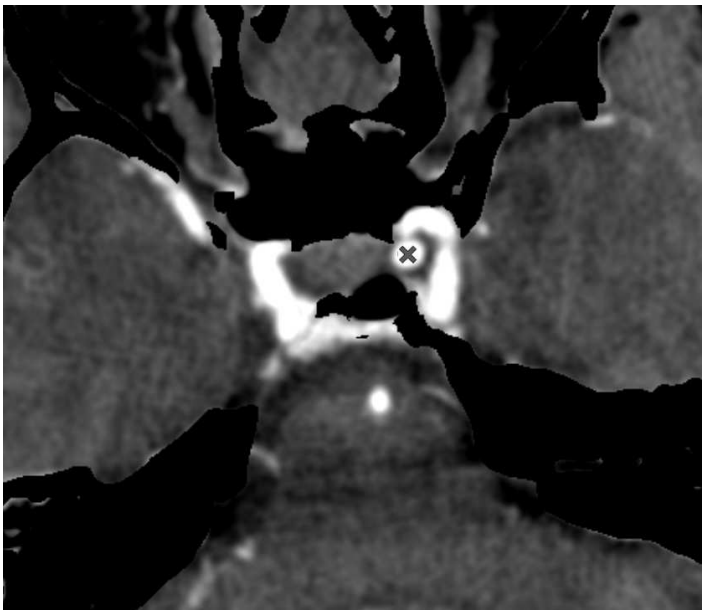

Figure 1. MPR of BSCTA of skull base: Start marker × (= seed) in aneurysm of left Carotissiphon.

The greyvalue of the seed is determined and a lower threshold for segmentation is adapted accordingly. Starting from the seed an adaptive region-growing in the 3D data set is implemented. In iterative steps voxels are segmented as follows: the 6-3D-neighbourhood of a start voxel is explored. In the first iteration the start voxel is the seed marked by the user, in all following iterations it is one of the voxels segmented in the previous

step. Neighbouring voxels with a greyvalue higher than the lower threshold are considered to be part of the region. They are recorded in a list as start voxels for the subsequent step. Once the entire neighbourhood of all current start voxels has been examined this iteration is completed. For the following iteration all voxels identified as start voxels in the previous step are treated in the same way (see Fig. 2).

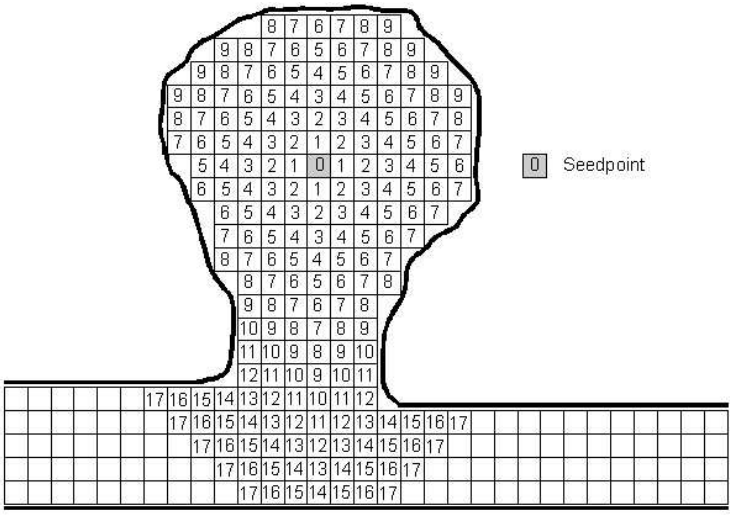

Figure 2. Process of segmentation in an aneurysm: Numbers match respective iterational step of segmentation, 0 = marker set by user.

In each step the number of newly found neighbouring voxels is recorded. This figure follows a typical behaviour: it increases at the beginning of the segmentation, reaches a maximum just before the volume of the aneurysm has been segmented entirely and then starts to decrease again (see Fig. 3). Once the segmentation reaches the vessels associated to the aneurysm the number of voxels segmented in each step drops to a local minimum (see step 12 in Fig. 2 and Fig. 3). This condition is employed as criterion for termination of the segmentation. All voxels segmented in the process, including the voxels of the last segmentation step, are considered to be associated to the aneurysm . They are kept in a data structure which can be made persistent for documentation purposes.

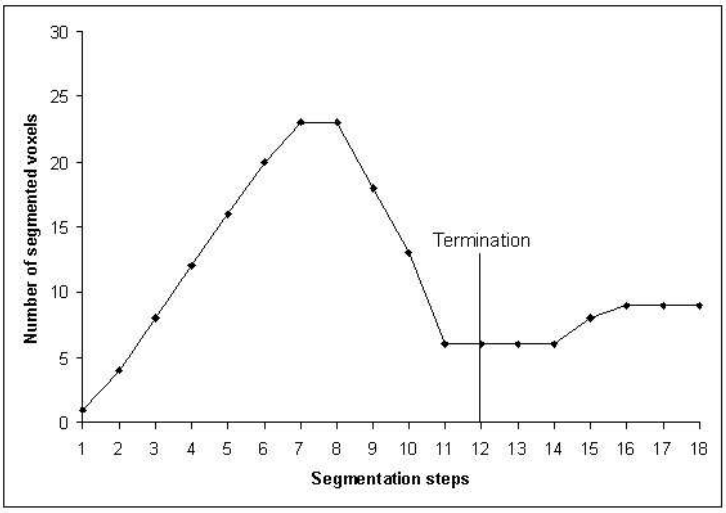

Figure 3. Process of segmentation in an aneurysm: Number of voxels segmented in each iteration.

The result of the segmentation can be blended into the MPR visualisation of a BSCTA image or can be visualised three-dimensionally (see Fig. 4). Thus the clinician is provided with the means to examine the aneurysm from various perspectives.

Figure 4. Result of segmentation of the marked aneurysm: Blended into MPR as grey area around start marker (left) and three-dimensional view of segmented aneurysm (right).

Blending the BSCTA image into a VRT visualisation is also possible and supports assessment of the topographic situation in the vicinity of the aneurysm (see Fig. 5).

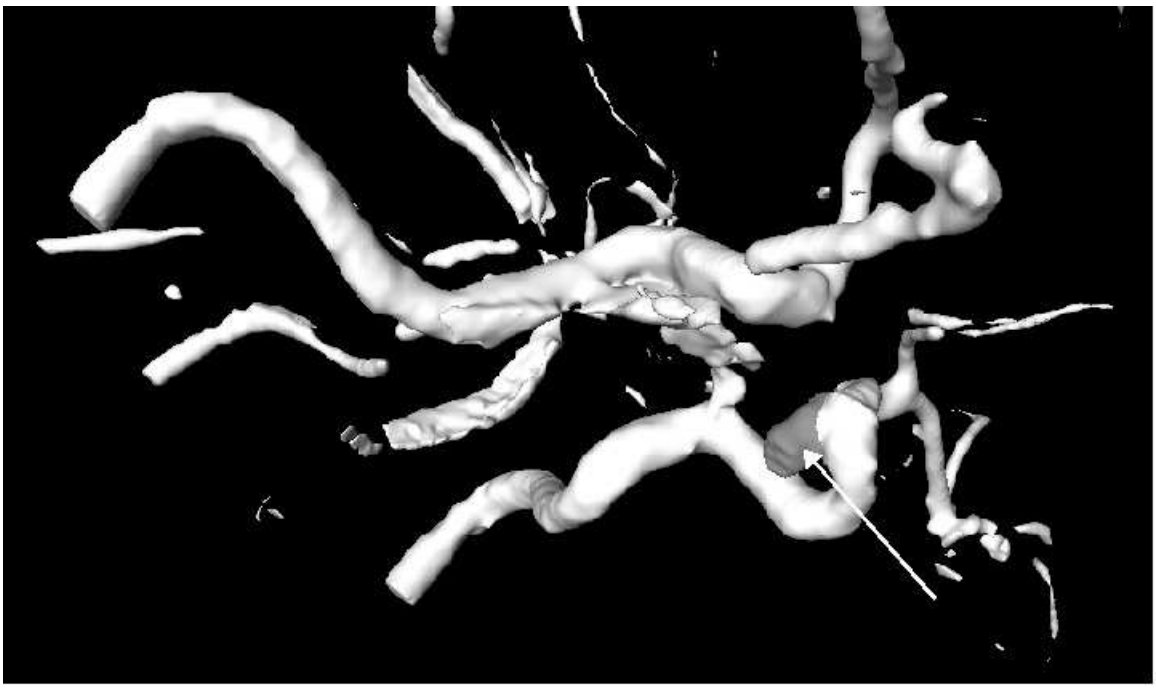

Figure 5. Result of segmentation of the marked aneurysm: Blended into VRT of vessels of the brain (→).

4.1.1 Computation of Diameter, Volume and Surface

As mentioned above, risk for rupture and diameter of an aneurysm correlate directly. Maximum and minimum diameter as well as volume and surface of the aneurysm can be computed from the result of the segmentation (see Fig. 6). The centre of gravity of the aneurysm is determined for calculation of the diameters. After that a number of rays sufficent to guarantee accurate results is projected from this point evenly in all spacial directions. The rays are extended until they touch the boundaries of the aneurysm. The length of two opposed rays is added up to the respective diameter. In case the centre of gravity is not situated in the segmented region it is shifted into the aneurysm before starting the calculation of the diameter. Shifting commences as follows: a ray in direction of the shortest distance between centre of gravity of the aneurysm and its border is generated. Then the centre of gravity is shifted along this ray until it is situated halfway between both piercing points of the ray through the surface of the aneurysm. The volume is calculated by multiplying the number of segmented voxels by volume per voxel. By generation of a winged-edge mesh on the outer layer of segmented voxels the surface extension of the aneurysm is computed.

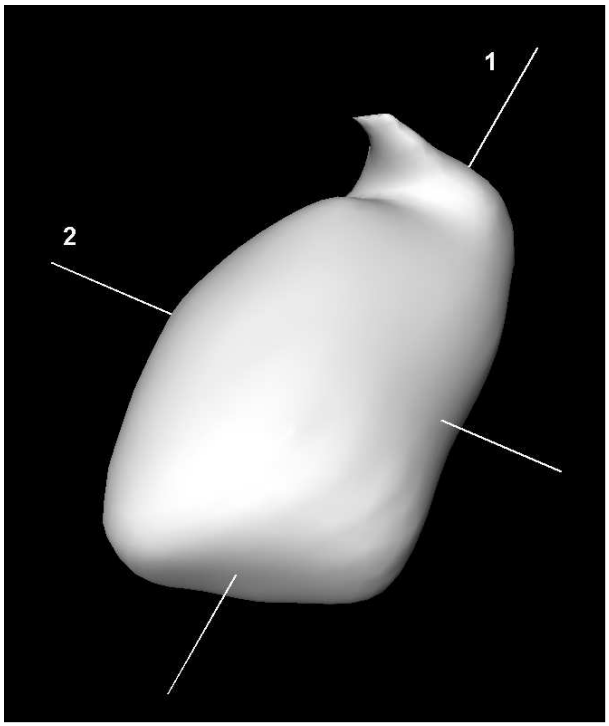

Figure 6. Maximum (1) and minimum (2) diameter of the aneurysm.

4.1.2 Associated Vessels

To define vessels associated to the segmented aneurysm the region growing is extended further. Termination ensues after a number of iterations set as default or pre-selected by the user. Likewise the segmentation process can be repeated to achieve the desired length of segmented vessel. Visualisation of the result allows for presentation of the aneurysm in context with vascular structures in close proximity. Segmentation of associated vessels is also essential for generation of wall models of the aneurysm and hence for haemodynamic modelling itself (see Fig. 7).

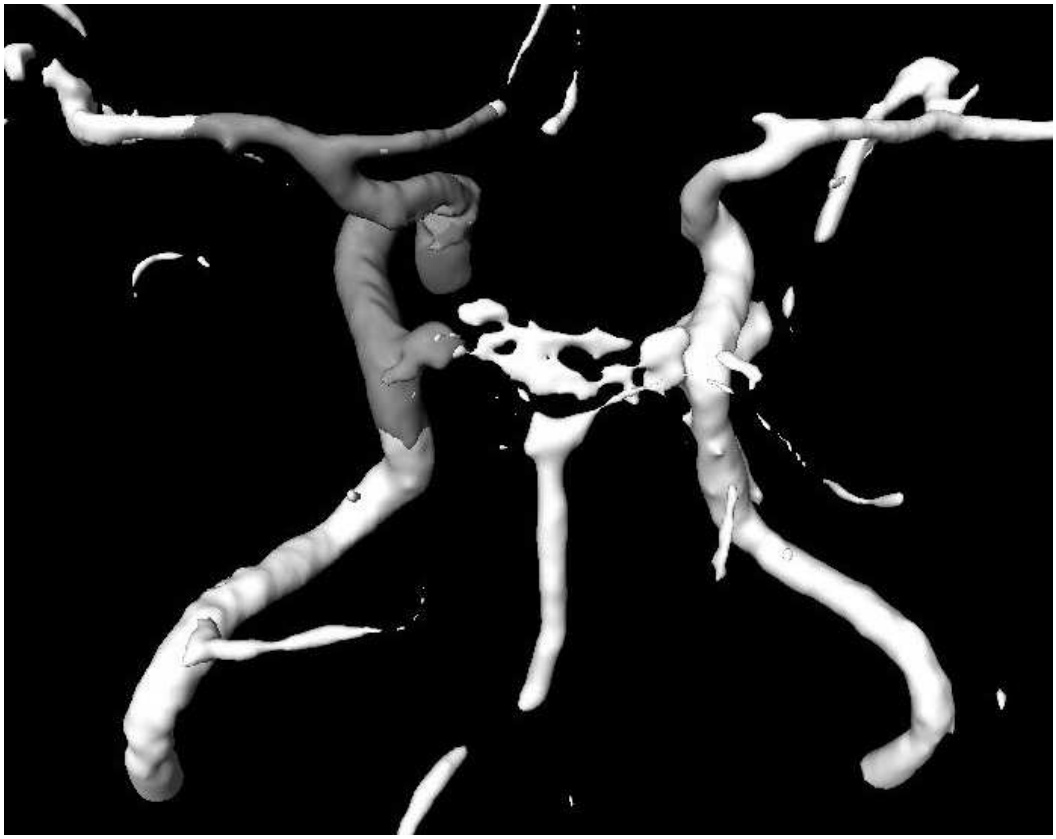

Figure 7. VRT of vessels in the brain including segmented aneurysm (dark grey) and associated vessels (middle grey).

4.2 Flow Modelling and Haemodynamics

An STL representing the geometry of the vascular wall of the aneurysm and its associated vessels is generated by means of a Marching Cubes Algorithm[28] from the segmentation produced in the previous step. By refining this mesh into a Delaunay triangulation and taking into account parameters of the vascular wall such as resiliency a realistic model of the vascular wall is generated. This model presents the fundamentals for computations of blood flow and haemodynamics inside the aneurysm. In particular values of major importance for research on therapeutic approaches and prognostic aspects like pressure onto vascular walls (see Fig. 8), wall shear stress (see Fig. 9) and pathlines of blood flow (see Fig. 10) are then computed based on this model. Furthermore a dynamic simulation of the blood flow in the aneurysm is carried out.

5. RESULTS

The proposed method requires only a single user-interaction to produce accurate segmentation of the respective aneurysm in all testcases. Termination of the process of segmentation ensues automatically just as the adjoining vessel is reached. Values of clinical importance such as diameter and volume of the aneurysm are calculated automatically based on the segmentation. Extension of the segmentation into associacted vascular structures provides for visualisation of the topographical situation in close proximity to the aneurysm. Based on this data a model of the vascular wall can be generated and applied to achieve realistic modelling of the haemodynamic situation in the aneurysm and vessels.

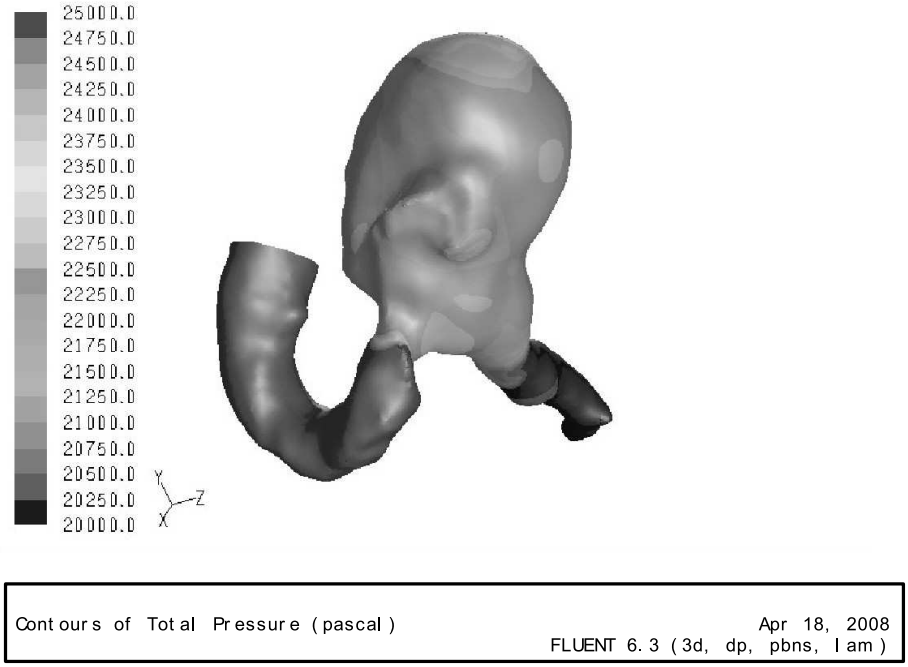

Figure 8. Haemodynamics: Total pressure of blood onto vascular wall of an aneurysm in Pascal (with courtesy of Ralf Kröger, ANSYS Fluent Inc., Germany).

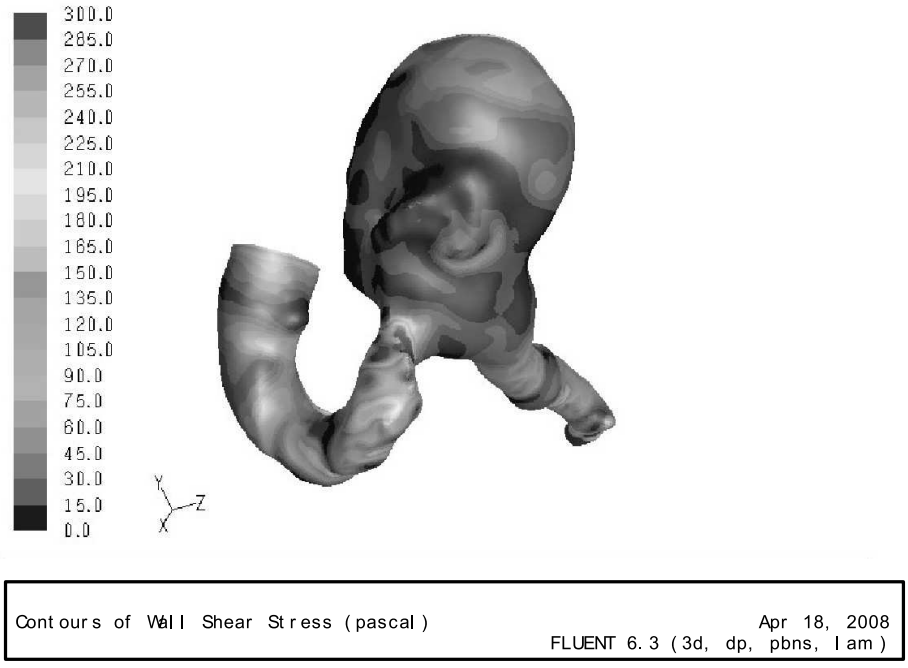

Figure 9. Haemodynamics: Wall shear stress onto vascular wall of an aneurysm in Pascal (with courtesy of Ralf Kröger, ANSYS Fluent Inc., Germany).

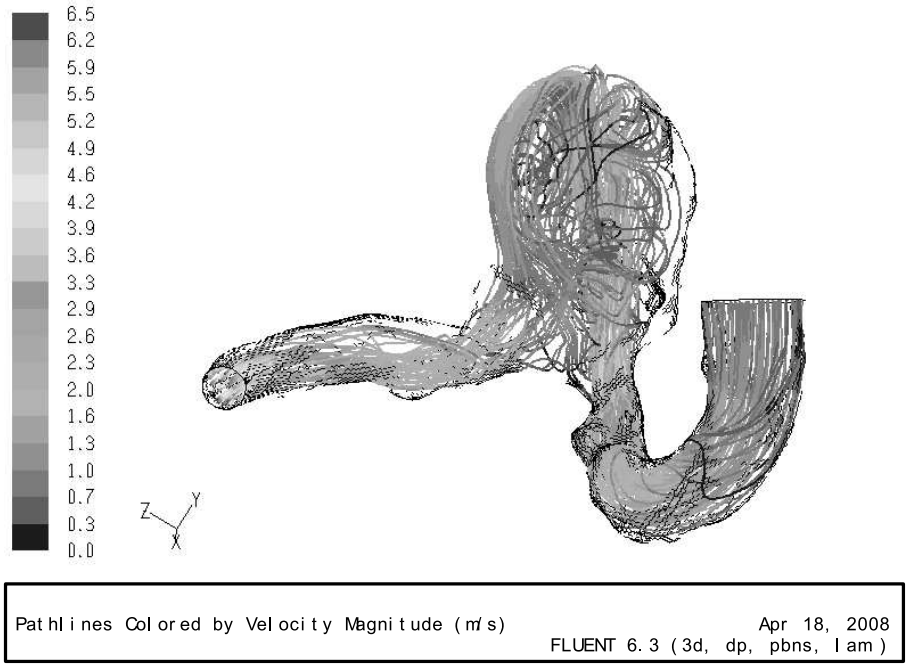

Figure 10. Haemodynamics: Pathlines of blood flow in an aneurysm (with courtesy of Ralf Kröger, ANSYS Fluent Inc., Germany).

6. CONCLUSIONS

The method presented in this work provides a powerful tool for accurate semi-automatic segmentation of intracranial aneurysms of various shapes, sizes and locations. Very important from a clinical point of view is that no additional scans besides the BSCTA standard scans are required. By setting a marker into the aneurysm and starting the application radiologist and surgeon receive precise information about important values of the aneurysms. As user-interaction is limited to the marking of the aneurysm the results of any values calculated on the basis of the segmentation become comparable and independent of the respective user. This is of paramount importance not only for clinical monitoring and risk assessment but also for intervention planning. Wall models of aneurysms and vessels are generated by means of STL meshes derived from the segmentation. Thus modelling of the haemodynamics is realised which itself is a crucial enhancement for future work addressing intervention planning and prognostic aspects not only of intracranial aneurysms.

7. FUTURE WORK

Employment of the presented method in conjunction with upcoming CAD techniques for automatic detection of aneurysms[29] enhances CAD substantially. Thus aneurysms could not only be detected automatically but at the same time clinically important values could be calculated automatically. First studies linking haemodynamics and risk for rupture of aneurysms have been presented[30] . This work contributes to future research in this field by providing techniques to segment aneurysms in widely available BSCTA standard scans and to create STL meshes suitable for flow modelling from these segmentations. The technique could be applied to implement retrospective studies supporting the evaluation of theoretical findings in haemodynamics of aneurysms by clinical evidence. Further methods aiming on intervention planning in the field of neurosurgery could be developed by applying the techniques developed for this paper. An example would be the support of the surgeon in the pre-operative adjustement of the coil or clip to be used for the invasive treatment of an aneurysm.

8. ACKNOWLEDGEMENTS

We would like to thank Ralf Kröger of ANSYS Fluent Inc., Darmstadt, Germany who kindly supplied the haemodynamic models displayed in this paper which are based on our segmentation data.

REFERENCES

[1] Wardlaw, J. and White, P., "The detection and management of unruptured intracranial aneurysms," *Brain* **123**, 205–221 (2000).

[2] White, P. and Wardlaw, J., "Unruptured intracranial aneurysms," *Journal of Neuroradiology* **30**, 336–350 (2003).

[3] Nahed, B., Seker, A., Guclu, B., Otzturk, A., Finberg, K., Hawkins, A., DiLuna, M., Lifton, R., and Gunel, M., "Mapping a mendelian form of intracranial aneurysm to 1p34.3-p36.13," *American Journal of Human Genetics* **76**(1), 172–179 (2005).

[4] Broderick, J., Sauerbeck, L., Foroud, T., III, J. H., Pankratz, N., Meissner, I., and Jr., R. B., "The familial intracranial aneurysm (fia) study protocol," *BMC Medical Genetics* , 6–17 (2005).

[5] Linn, F., Rinkel, G., Algra, A., and van Gijn, J., "Incidence of subarachnoid hemorrhage," *Stroke* **27**, 625–629 (1996).

[6] Juvela, S., "Hypertension and aneurysmal subarachnoid hemorrhage," *Wiener Klinische Wochenschrift* **114**, 285–286 (May 2002).

[7] Juvela, S., "Natural history of unruptured intracranial aneurysms: risks for aneurysm formation, growth, and rupture," *Acta Neurochirurgica Supplement* **82**, 27–30 (2002).

[8] Ohkuma, H., Tabata, H., Suzuki, S., and Islam, M., "Risk factors for aneurysmal subarachnoid hemorrhage in aomori, japan," *Stroke* **34**, 96–100 (2003).

[9] Juvela, S., "Treatment options of unruptured intracranial aneurysms," *Stroke* **35**, 372–374 (2004).

[10] Juvela, S., Porras, M., and Poussa, K., "Natural history of unruptured intracranial aneurysms: probability and risk factors for aneurysm rupture," *Journal of Neurosurgery* **93**(3), 379–387 (2000).

[11] van Gijn, J. and Rinkel, G., "Subarachnoid haemorrhage: diagnosis, causes, management," *Brain* **124**, 249–278 (2001).

[12] Kirkpatrick, P., "Subarachnoid haemorrhage and intracranial aneurysms: what neurologists need to know," *Journal of Neurology, Neurosurgery and Psychiatry* **73**(Supplement 1), i28–i33 (2002).

[13] King, J. J., "Epidemiology of aneurysmal subarachnoidal hemorrhage," *Neuroimaging Clinics of North America* **7**(4), 659–668 (1997).

[14] Esteban, J. and Cervera, V., "Perfusion CT and angio CT in the assessment of acute stroke," *Neuroradiology* **46**, 705–715 (2004).

[15] Thurnher, M. and Castillo, M., "Imaging in acute stroke," *European Radiology* **15**, 408–415 (2005).

[16] Tomandl, B., Klotz, E., Handschu, R., Stemper, B., Reinhardt, F., Huk, W., Eberhardt, K., and Fateh-Moghadam, S., "Comprehensive imaging of ischemic stroke with multisection CT," *Radiographics* **23**, 565–592 (2003).

[17] Lell, M., Anders, K., Klotz, E., Ditt, H., W., W. B., and Tomandl, B., "Clinical evaluation of bone subtraction CT angiography (BSCTA) in head and neck imaging," *European Radiology* **16**, 889–897 (2006).

[18] Tang, P.-H., Hui, F., and Sitoh, Y.-Y., "Intracranial aneurysm detection with 3t magnetic resonance angiography," *Annals of the Academy of Medicine, Singapore* **36**, 388–393 (Jun 2007).

[19] Adams, W. M., Laitt, R. D., and Jackson, A., "The role of MR angiography in the pretreatment assessment of intracranial aneurysms: A comparative study," *American Journal of Neuroradiology* **21**, 1618–1628 (Oct 2000).

[20] Zhu, W., Feng, D., Qi, J., Xia, L., and Wang, C., "Evaluation of large intracranial aneurysms with cine MRA and 3D contrast-enhanced MRA," *Journal of Huazhong University of Science and Technology* **24**(1), 95–98 (2004).

[21] Yan, P. and Kassim, A., "Segmentation of volumetric MRA images by using capillary active contour," *Medical Image Analysis* **10**(3), 317–329 (2006).

[22] Chung, A., Noble, J., and Summers, P., "Vascular segmentation of phase contrast magnetic resonance angiograms based on statistical mixture modeling and local phase coherence," *IEEE Transactions on Medical Imaging* **23**, 1490–507 (Dec 2004).

[23] Lell, M., Anders, K., Klotz, E., Ditt, H., Bautz, W., and Tomandl, B., "Clinical evaluation of bone subtraction CT angiography (BSCTA) in head and neck imaging," *European Radiology* **16**, 889–897 (2006).

[24] Tomandl, B., Hammen, T., Klotz, E., Ditt, H., Stemper, B., and Lell, M., "Bone-subtraction CT angiography for the evaluation of intracranial aneurysms," *American Journal of Neuroradiology* **27**, 55–59 (2006).

[25] Venema, H., Hulsmans, F., and den Heeten, G., "CT angiography of the circle of willis and intracranial internal carotid arteries: maximum intensity projection with matched mask bone elimination-feasibility study," *Radiology* **218**, 893–898 (2001).

[26] Lell, M., Ditt, H., Panknin, C., Sayre, J., Ruehm, S., Klotz, E., and Villablanca, B. T. J., "Bone-subtraction CT angiography: evaluation of two different fully automated image-registration procedures for interscan motion compensation," *American Journal of Neuroradiology* **28**(7), 1362–1368 (2007).

[27] Urschler, M., Ditt, H., and Bischof, H., "Partially rigid bone registration in CT angiography," *Computer Vision Winter Workshop 2006, Czech Pattern Recognition Society* , 1–6 (2006).

[28] Lorenson, W. and Cline, H., "Marching cubes: A high resolution 3D surface reconstruction algorithm," *Proceedings of SIGGRAPH* , 163–169 (1987).

[29] Uchiyama, Y., Ando, H., Yokoyama, R., Hara, T., Fujita, H., and Iwama, T., "Computer-aided diagnosis theme for detection of unruptured intracranial aneurysms in MR angiography," *Proc. of 27th Annual International Conference on Engineering in Medicine and Biology* **1**, 3031–3034 (2005).

[30] Castro, M., Putman, C., Radaelli, A., Frangi, A., and Cebral, J., "Image-based investigation of hemodynamics and rupture of cerebral aneurysms of a single morphological type: Terminal aneurysms," *Proc of SPIE* **6916** (2008).